Improved numerical simulation of electromagnetic wave scattering from perfectly conducting random surfaces

Y. Oh
K. Sarabandi

Indexing terms: Electromagnetic wave scattering, Simulation, Numerical analysis, Monte Carlo simulation

Abstract: A Monte Carlo simulation of electromagnetic scattering from one-dimensional perfectly conducting random surfaces is considered in the paper. Surface profiles of desired statistics are generated numerically using a standard procedure and the scattering solution for the surface samples of finite length is calculated using the method of moments. A new technique is used to reduce the effect of the edges of the finite surface samples. In this technique, the conductivities of the surface near edges are controlled by adding an appropriate tapered resistive sheet. It is shown that the accuracy at large angles of incidence, $\theta > 50°$, and the computation efficiency are improved significantly using this method, when compared to the standard tapered illumination method. Results based on this numerical approach are compared with those based on the small perturbation and physical optics approximations in their respective regions of validity.

1 Introduction

Numerical simulation of electromagnetic scattering from a one-dimensional perfectly conducting random surface is of interest [1–7], for its application as a benchmark in evaluating approximate theoretical models and a complementary solution to the theoretical models when they fail. Although numerical solutions for scattering problems are considered to be 'exact', their accuracy becomes limited when applied to rough surfaces. Rough surfaces are targets of infinite extent, hence approximations to the geometry or the formulation of the problem must be considered to make the numerical solution tractable. The standard method to suppress the effect of the edges of a finite surface sample is the tapered illumination approximation. In this approach, the method of moments is applied to surface samples, assuming that the incident wave has a Gaussian amplitude variation, and the scattering coefficients are calculated from the second moments of the scattered field normalised by the illumination integral. The beamwidth of the tapered illumination should be narrow, to suppress the edge contributions at large angles of incidence, which results in an inaccurate solution by excessive smoothing, especially for a relatively smooth random surface with a large correlation length. Therefore, the beamwidth of the tapered illumination should be chosen carefully, according to the incidence angle and the sample width. The tapered illumination approximation is numerically inefficient, because the effective width of the sample surface contributing to the scattered field, is much smaller than the width of the surface used in the numerical calculation.

In this paper, the contribution from the edges of the surface samples to the scattered field is minimised by controlling the conductivity of the surface near each edge by adding an appropriate tapered resistive sheet. It is shown that the addition of a short length of a tapered resistive sheet (1λ) at each end of surface sample can suppress the edge contribution significantly, at even large angles of incidence. Scattering simulations based on the new technique show a good agreement with the classical scattering models, the small perturbation method and the physical optics model, at their regions of validity. The backscattering coefficient predicted by the new technique is accurate for incidence angles as high as 80°, while the angular validity range of the standard method is limited to lower incidence angles. This is particularly the case for relatively smooth surfaces with large correlation length ($ks < 1.0$, $kl > 6.0$ where k is wavenumber, s is the RMS height and l is the correlation length).

2 Formulation

The scattered field data from a one-dimensional conducting surface are obtained by a Monte Carlo simulation. Basically scattered fields from a large number of randomly generated sample surfaces are computed numerically, and are used to estimate the backscattering coefficient of the random surface. First, the surface current density $\mathbf{J}_e$, on each surface sample excited by a planewave, is determined using the method of moments (MoM). For a horizontally polarised wave, the electric-field integral equation (EFIE) and, for a vertically polarised wave, the magnetic-field integral equation (HFIE) is used, respectively. The EFIE and HFIE are

IEE Proceedings online no. 19971189

Paper first received 28th October 1996 and in revised form 10th February 1997

Y. Oh is with the Department of Radio Science and Engineering, Hong-Ik University, Seoul, Korea

K. Sarabandi is with the Department of Electrical Engineering and Computer Science, The University of Michigan, Ann Arbor, USA

given, respectively, by

$$\mathbf{E}^i(\bar{\rho}) = \frac{k_0 Z_0}{4} \int_l \mathbf{J}_e(\bar{\rho}) H_0^{(1)}(k_0|\bar{\rho} - \bar{\rho}'|)dl' \quad (1)$$

$$-\hat{n} \times \mathbf{H}^i(\bar{\rho}) = -\frac{1}{2}\mathbf{J}_e(\bar{\rho}) + \frac{i}{4} \int_l \hat{n} \times \{\mathbf{J}_e(\bar{\rho}') \times \nabla' H_0^{(1)}(k_0|\bar{\rho} - \bar{\rho}'|)\}dl' \quad (2)$$

Here k_0 is the wavenumber, Z_0 is the intrinsic impedance of free space, $H_0^{(1)}$ is the zeroth-order Hankel function of the first kind, $\hat{n}$ is the unit normal vector of the surface, and ρ and ρ' are the position vectors of observation and source points, respectively. After a sample surface is discretised into sufficiently small cells, eqns. 1 and 2 are cast into matrix equations using the pulse-basis function and point-matching technique.

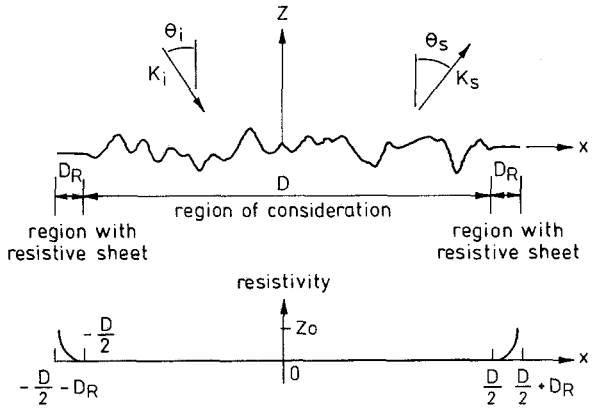

Fig. 1 *Sample surface loaded with resistive sheets, and resistivity function profile*

The surface current induced by a horizontally polarised incidence wave exhibits the familiar singularity near the edges of the surface, which has a significant effect on the backscattered field away from normal incidence. However, this is not the case for the vertically polarised incidence wave for a one-dimensional perfectly conducting surface. To suppress the singular behaviour of the current near the edges, a tapered resistive sheet is added to each end of the surface sample as shown in Fig. 1. Using the following boundary conditions for resistive sheets [8],

$$[\hat{n} \times \mathbf{E}]_-^+ = 0, \qquad \hat{n} \times (\hat{n} \times \mathbf{E}) = -R\mathbf{J} \quad (3)$$

the integral equation for horizontal polarisation becomes

$$\mathbf{E}^i(\bar{\rho}) = R(\bar{\rho})\mathbf{J}_e(\bar{\rho}) + \frac{k_0 Z_0}{4} \int_l \mathbf{J}_e(\bar{\rho}) H_0^{(1)}(k_0|\bar{\rho} - \bar{\rho}'|)dl' \quad (4)$$

where R is the resistivity of the surface. Eqn. 4 applies over all of the surface and is cast into a matrix equation [Z] [I] = [V] using the point matching technique. The elements of the impedance matrix can be obtained from

$$z_{mn} \approx R(x_n, y_n)\delta_{mn} + \frac{k_0 Z_0}{4} \int_{\Delta x_n} H_0^{(1)}\left(k_0\sqrt{(x_m - x_n)^2 - (z_m - z_n)^2}\right) \times \sqrt{1 + \left(\frac{dz_n}{dx_n}\right)^2} dx_n \quad (5)$$

where δ_{mn} is the Kronecker delta function, while the elements of the excitation vector [V] are given by

$$v_m = \exp[ik_0(\sin\theta_i x_m - \cos\theta_i z_m)] \quad (6)$$

The small argument expansion of the Hankel function is used in the evaluation of the diagonal elements of the impedance matrix. The nondiagonal elements, $z_{mn}(m \neq n)$, are obtained by evaluating the integral in eqn. 5 numerically, using a four-point Gaussian-quadrature integration technique.

The resistivity profile, $R(x)$, plays an important role in suppression of the edge current. The objective is to suppress the singular behaviour of the current, using a resistivity profile over the smallest possible width. Using trial and error, the following resistivity profile was chosen:

$$R(x) = \begin{cases} 0 & |x| \leq \frac{D}{2} \\ Z_0\left(\frac{D/2 - |x|}{D_R}\right)^4 & \frac{D}{2} \leq |x| \leq \frac{D}{2} + D_R \end{cases} \quad (7)$$

where D is the width of the sample surface and D_R is the width of the resistive section.

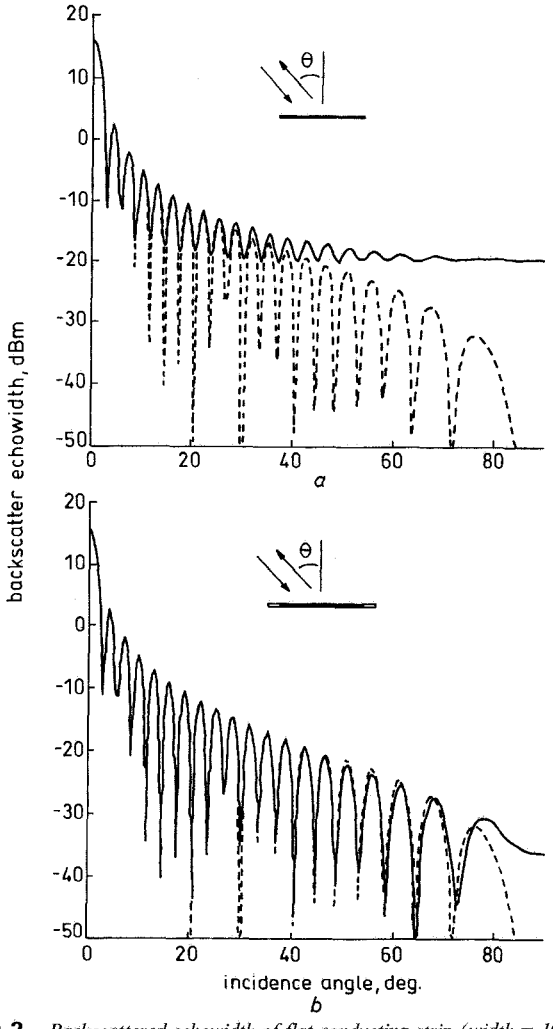

Fig. 2 *Backscattered echowidth of flat conducting strip (width = 10 λ)*
a Without resistive sheets
b With resistive sheets of length 1λ at each side
——— HH-pol
– – – – VV-pol

To illustrate the effect of edge current on backscatter, scattering from a flat conducting surface with a width of 10λ is considered. The radar-backscattering echowidth (two-dimensional radar cross-section) of the conducting strip is shown in Fig. 2*a* for both polarisa-

tions. The effect of edge current on echowidth becomes important away from normal incidence for horizontal polarisation. Fig. 2*b* shows the backscattering echowidth of the same conducting strip, when resistive sheet segments (1λ) are added to both edges of the conducting strip. In this case, the backscattering echowidth for horizontal polarisation decreases with incidence angle, in a manner similar to the echowidth for vertical polarisation, which clearly indicates the suppression of the edge currents.

Tapered resistive sheets were not used for the case of vertical polarisation. For vertical polarisation where the electric field is perpendicular to the edges of the surface samples, the excessive edge current must go to zero near the edges. Therefore, no significant backscatter can be attributed to the edges of the finite samples for vertical polarisation.

3 Verification of the new numerical technique

To demonstrate the validity of the numerical simulation, the sample surfaces with desired roughness statistics are generated using a standard approach [1, 2]. First, a random number string is generated for a Gaussian height distribution with zero mean and standard deviation of 1. Then, the Gaussian distribution is correlated with a correlation function. In this paper, a Gaussian correlation function having a correlation length l is correlated with the Gaussian distribution, N [0, 1], and the desired standard deviation (RMS height) s is multiplied by the surface height distribution to obtain desired roughness ks and kl, where k is wavenumber.

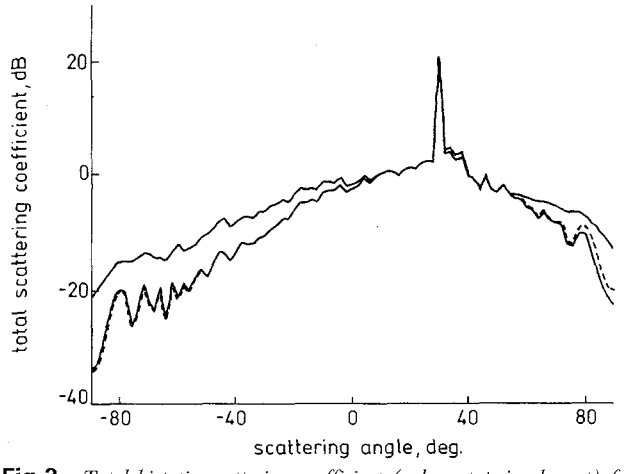

Fig. 3 *Total bistatic scattering coefficient (coherent + incoherent) for surface with ks = 0.3 and kl = 3.0*
Both polarisations are shown for incidence angle $\theta_i = 30°$ and the effect of the width of tapered resistive sheet is also examined. Resistive sheet length:
——— 1λ, VV-pol
– – – – 3λ, HH-pol

Fig. 3 shows the bistatic scattering coefficient for a Gaussian surface with $ks = 0.3$ and $kl = 3.0$, for both of VV- and HH-polarisations at 30° incidence angle. The Figure also shows the effect of the length of the resistive sheet for the HH-polarisation response. The solid and dotted line curves show the bistatic response when a resistive sheet of length 1λ and 3λ is used, respectively. It is shown that the difference between the scattering patterns are negligible. In the computation of the bistatic response, the sample width $D = 30\lambda$ and the number of independent samples $N = 40$ were used. The sample surfaces in the following examples are all loaded with a short tapered resistive sheet of width 1λ. When the sample surface width is 30λ, for example, a surface of total length 32λ, including 1λ resistive sheets, at both ends is used for the computation of the surface current induced by the planewave excitation. The currents induced over the resistive sheets are excluded from computation of the scattered field.

The small perturbation method (SPM) is known to be valid when $ks < 0.3$, $kl < 3.0$ and $m < 0.3$. Here, m is the RMS slope and is given by $m = \sqrt{2}s/l$, for a surface with a Gaussian correlation function. The backscattering coefficients from a surface with $ks = 0.15$ and $kl = 2.0$ are computed using the SPM and compared with the MoM solution, as shown in Fig. 4. For the numerical computation of the backscattering coefficients, the sampling interval $\Delta x = 0.1\lambda$, the sample width $D = 14\lambda$ and the number of independent samples $N = 40$ were used. Fig. 4 shows that the SPM solution agrees very well with the MoM solution for incidence angles as high as 80°.

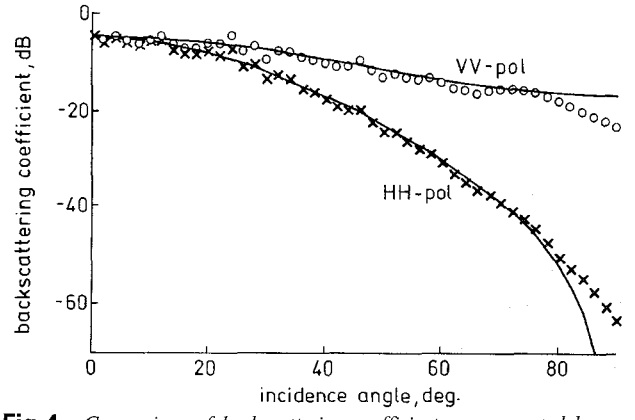

Fig. 4 *Comparison of backscattering coefficients as computed by new numerical technique and first-order small-perturbation solution*
For a surface with $ks = 0.15$ and $kl = 2.0$
($N = 40$, $D = 14\lambda$, $\Delta x = 0.1\lambda$)
——— SPM model
O, × MoM with resistive sheets

The physical optics (PO) model can also be used to examine the validity of the numerical simulation at the other extreme roughness conditions. There are various PO solutions in the literature. For example, the PO model which appeared in [9, 11] is formulated by approximating the ensemble average within the diffraction integral, by ignoring all local slope terms. Another familiar form of PO model is given in [12], which is formulated by including the first-order local slope term and ignoring 'edge effect' contribution. Instead of using those models, a new PO model in [13] is used in this paper to be compared with the MoM solution. The new PO model is formulated exactly by employing the spectral representation of the delta function and the characteristic function of a Gaussian random vector [13]. As the PO solution of the surface backscattering is proportional to the Fresnel reflectivity, the backscattering coefficients from perfectly conducting surfaces computed by the PO model do not show a difference between VV- and HH-polarisations as shown in Fig. 5. Fig. 5 compares the backscattering coefficients as computed by the new PO model and the new numerical (MoM) technique with resistive sheets for both polarisations. The roughness parameters of the surface are $ks = 1.0$ and $kl = 8.0$ which fall at the margin of the validity region of PO model ($l > \lambda$, $m < 0.25$ [9]). In this numerical simulation, the following parameters were used: $\Delta x = 0.2\lambda$, $D = 30\lambda$ and $N = 40$. The PO solution agrees very well with the MoM solution over a wide

range of incidence angles ($0° < \theta < 70°$). As the MoM with resistive sheets agrees very well with the SPM and the PO model at their validity regions, it is reasonable to expect that the numerical simulation can accurately predict the statistics of the scattered field for surfaces with intermediate roughness conditions.

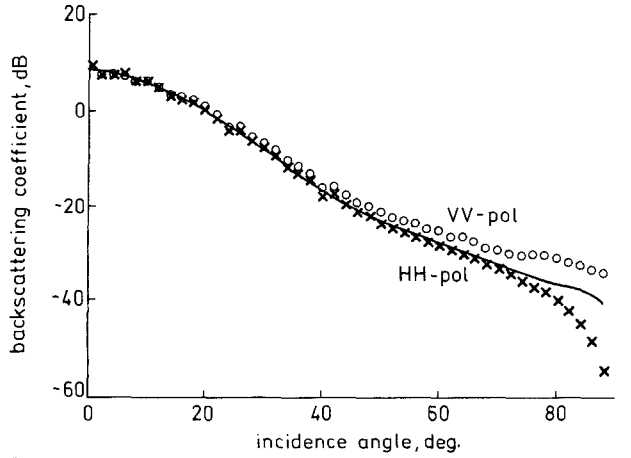

Fig. 5 *Comparison of backscattering coefficients as computed by new numerical method and new formulation of Kirchhoff approximation*
For a surface with $ks = 1.0$ and $kl = 8.0$
($N = 40$, $D = 30\lambda$, $\Delta x = 0.2\lambda$)
——— New PO model
○, × MoM with resistive sheets

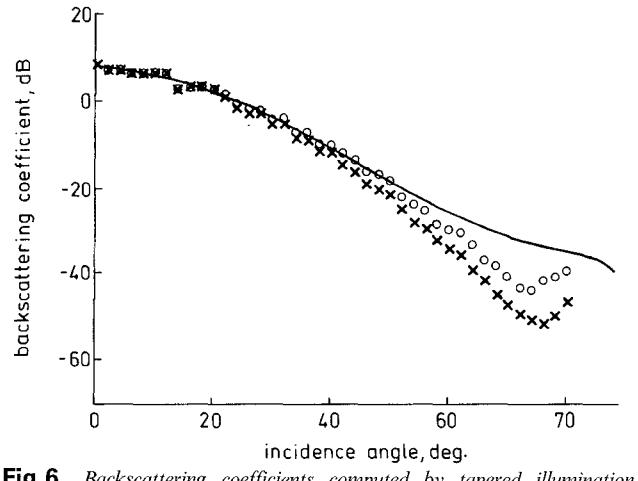

Fig. 6 *Backscattering coefficients computed by tapered illumination method and new formulation of Kirchhoff approximation*
For a surface with $ks = 1.0$ and $kl = 6.13$
($N = 40$, $D = 30\lambda$, $\Delta x = 0.2\lambda$)
——— New PO model
○ MoM, VV-pol, tapered illumination
× MoM, HH-pol, tapered illumination

4 Comparison with other numerical techniques

To demonstrate the efficiency of the new numerical technique, a comparison with existing numerical techniques is necessary. The most widely used numerical technique is based on the method of moments in conjunction with a tapered incident illumination [7]. The backscattering coefficients of the random surface with $ks = 1.0$ and $kl = 6.13$ are computed using the Gaussian-tapered illumination technique for comparing with the solution obtained by the new numerical technique. Fig. 6 shows the comparison between the new PO model and the tapered illumination technique. In this comparison, the taper function is given by [7]

$$E^i(\bar{\rho}) = \exp\left[i\bar{k}_i \cdot \bar{\rho}\{1 + w(\bar{\rho})\} - \frac{(x - z\tan\theta_i)^2}{g^2}\right]$$

$$w(\bar{\rho}) = \frac{2(x - z\tan\theta_i)^2/g^2 - 1}{(kg\cos\theta_i)^2} \qquad (8)$$

where $k\cdot\rho = k_0(\sin\theta_i x - \cos\theta_i z)$, θ_i is the incidence angle and g is a constant parameter controlling the tapering of the illumination. The resulting scattering coefficient is the ratio of scattering cross-section normalised and the effective surface width L_{eff} given by

$$L_{eff} = \sqrt{\pi/2}g\left[1 - \frac{0.5(1 + 2\tan^2\theta_i)}{(k_0 g\cos\theta_i)^2}\right] \qquad (9)$$

In this numerical computation, g is chosen to be $g = 0.25D$, $D = 30\lambda$, $\Delta x = 0.2\lambda$ and $N = 40$. The backscattering coefficient computed by the Gaussian-tapered illumination method agrees well with the new PO model at small incidence angles ($0° < \theta_i < 50°$), however it predicts lower values for both polarisations at large incidence angles ($\theta_i > 50°$), as shown in Fig. 6. Comparison of Figs. 5 and 6 clearly shows the new numerical method is more accurate than the standard method over a wide range of incidence angles.

Fig. 6 shows that the backscattering coefficients are increasing over the angular range $75° < \theta_i < 90°$. The reason for this is that the second term, including $(k_0 g \cos\theta_i)^2$ in eqn. 9 is not small enough to be neglected at large incidence angles. In addition, at large incidence angles, the taper function could not eliminate the effect of the currents induced at the edges significantly, and, therefore, the backscatter contribution from the edges are observable. Therefore, as the incidence angle increases, the sample surface width as well as the inverse of g ($1/g$) should be increased, which makes the numerical solution inefficient.

It should be noted that the effective surface width of the tapered illumination technique is much smaller than the physical width. For example, when $g = 0.25\ D$ is used in eqn. 9, L_{eff} is about 31% of the physical width, while the effective width of samples in the new simulation with 1λ resistive sheets is about 94% of the physical width when $D = 30\lambda$. The scattered field is dominated by the contribution from the current induced over the effective width of a surface sample. Fig. 7 shows the comparison of the normalised current distributions on a typical surface sample as computing by the new and the tapered illumination techniques.

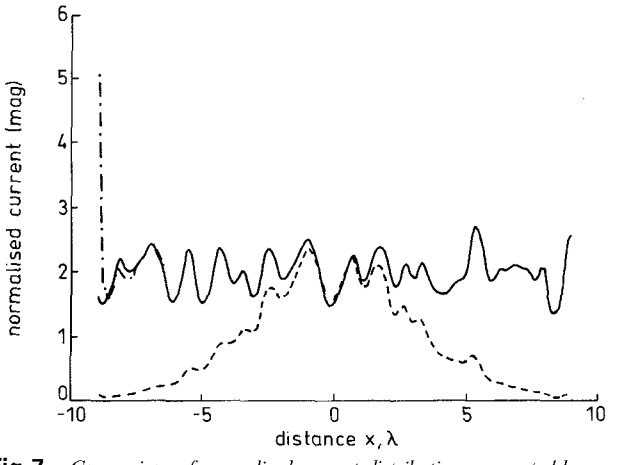

Fig. 7 *Comparison of normalised current distributions computed by new numerical technique and tapered illumination technique*
On a surface sample with $ks = 0.3$ and $kl = 3.0$ at 45° incidence angle
($D = 18\lambda$, $\Delta x = 0.1\lambda$)
——— New technique with resistive sheets
– – – – Tapered illumination technique
— · — Without resistive sheets

Another drawback of the tapered illumination technique is the lack of a systematic approach to select g. Fig. 8 shows the comparison of σ^0_{hh} between the new

technique and the tapered illumination technique, for various values of the parameter g for the surface with $ks = 1.0$ and $kl = 6.13$. The two numerical methods agree at low angles of incidence ($0° < \theta_i < 50°$), however the backscattering coefficients computed by the tapered illumination technique predict conflicting results for $\theta_i > 50°$, as the parameter g varies from $0.5D$ to $0.25D$. Worse results were obtained when other types of tapering functions were used, as suggested in [1, 2].

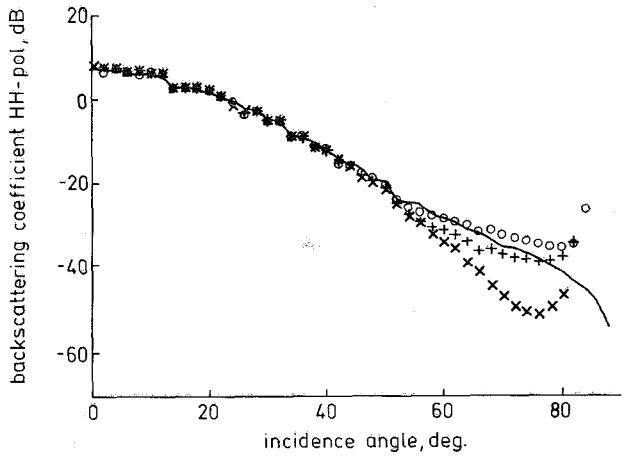

Fig. 8 *Backscattering coefficients (σ^0_{hh}) computed by new numerical technique and tapered illumination technique*
With various values of the tapering parameter g (0.25 D, 0.375 D, and 0.5 D) for a surface with $ks = 1.0$ and $kl = 6.13$
($N = 40$, $D = 30\lambda$, $\Delta x = 0.2\lambda$)
——— New numerical technique
○, +, × Tapered illumination technique
○ $g = 0.5D$
\+ $g = 0.375D$
× $g = 0.25D$

5 Conclusions

A Monte Carlo simulation comprised of a random surface generator, in conjunction with the method of moments, is developed to obtain the scattering statistics of one-dimensional conducting random surfaces. A new approach is introduced which efficiently eliminates the effect of edge currents on the finite sample surfaces. By adding a resistive sheet to each end of the sample surface, the edge currents are suppressed. The numerical simulations using the resistive loaded surface samples agree very well with the existing theoretical models (SPM and PO) in their regions of validity. The new method offers two major advantages over the standard tapered illumination method: (*a*) it is numerically more efficient, i.e. for a given accuracy the new method requires samples with smaller physical width, and (*b*) it has a wider angular range of validity which is independent of ks, kl and any uncertain parameter like 'g' employed in the tapered illumination technique.

6 Acknowledgments

This study was supported by NASA under contract NAGW-2125 and the Korean Agency of Defense Development.

7 References

1 AXLINE, R.M., and FUNG, A.K.: 'Numerical computation of scattering from a perfectly conducting random surface', *IEEE Trans. Antennas Propag.*, 1978, **AP–26**, (5), pp. 482–488
2 FUNG, A.K., and CHEN, M.F.: 'Numerical simulation of scattering from simple and composite random surfaces', *J. Opt. Soc. Am. A*, 1985, **2**, pp. 2274–2284
3 LENTZ, R.R.: 'A numerical study of electromagnetic scattering from ocean-like surfaces', *Radio Science*, 1974, **9**, pp. 1139–1146
4 NIETO-VESPERINAS, M., and SOTO-CRESPO, J.M.: 'Monte Carlo simulations for scattering of electromagnetic waves from perfectly conductive random rough surfaces', *Opt. Lett.*, 1987, **12**, pp. 979–981
5 DURDEN, S.L., and VESECKY, J.F.: 'A numerical study of the separation wavenumber in the two-scale scattering approximation', *IEEE Trans. Geosci. Remote Sensing*, 1990, **28**, pp. 271–272
6 RODRIGUEZ, E., KIM, Y., and DURDEN, S.L.: 'A numerical assessment of rough surface scattering theories, I. Horizontal polarization, II. Vertical polarization', *Radio Science*, 1992, **27**, pp. 497–527
7 THORSOS, E.: 'The validity of the Kirchhoff approximation for rough surface scattering using a Gaussian roughness spectrum', *J. Acoust. Soc. Am.*, 1988, **83**, (1), pp. 78–92
8 SENIOR, T.B.A.: 'Scattering by resistive strips', *Radio Sci.*, 1979, **14**, pp. 911–924
9 ULABY, F.T., MOORE, M.K., and FUNG, A.K.: 'Microwave remote sensing, active and passive, vol. 2' (Artech House, Norwood, MA, 1986)
10 CHEN, M.F., and FUNG, A.K.: 'Numerical study of validity of the Kirchhoff and Small-perturbation rough surface scattering models', *Radio Science*, 1988, **23**, pp. 163–170
11 TSANG, L., KONG, J.A., and SHIN, R.T.: 'Theory of microwave remote sensing' (John Wiley and Sons, New York, 1985)
12 BECKMANN, P., and SPIZZICHINO, A.: 'The scattering of electromagnetic waves from rough surfaces' (Pergamon Press, New York, 1979)
13 OH, Y.: 'An exact evaluation of Kirchhoff approximation for backscattering from a one-dimensional rough surface'. IEEE AP–S International Symposium, Baltimore, USA, July 1996, Vol. Digest 3, pp. 1522–1525